Lucent Patellar Lesions: A Pictorial Review

Ziang Lu[1*], Kira Chow[2], Benjamin Levine[1], Kambiz Motamedi[1], Joshua Leeman[2]

1. Department of Radiological Sciences, University of California Los Angeles, Los Angeles, California, USA

2. Musculoskeletal Section, Imaging Department, West Los Angeles Veterans Affairs, Los Angeles, California, USA

* **Correspondence:** Ziang Lu, Department of Radiological Sciences, University of California Los Angeles, Los Angeles, California, USA (*zianglu@mednet.ucla.edu*)

Radiology Case. 2022 Jun; 16(6):18-29 :: DOI: 10.3941/jrcr.v16i6.4484

ABSTRACT

A radiographically lucent patellar lesion may represent a variety of etiologies, ranging from more commonly seen degenerative, metabolic, infectious, developmental, posttraumatic, postoperative causes to rarer benign and malignant neoplasms. Clinical symptoms, surgical history, laboratory values, and radiographic features may help narrow the differential. In addition, radiographic features such as circumscribed borders and sharply delineated margins favor benign lesions while ill-defined margins suggest malignant etiologies. This case series illustrates the imaging findings and explores relevant clinical findings in a variety of interesting lucent patellar lesions.

REVIEW ARTICLE

REVIEW

A radiographically lucent patellar lesion may represent a variety of etiologies, ranging from more commonly seen degenerative, metabolic, infectious, developmental, posttraumatic, postoperative causes to rarer benign and malignant neoplasms. Subchondral cysts or erosions along the patellar articular surface are often related to underlying arthropathy such as osteoarthritis, gout, calcium pyrophosphate deposition, rheumatoid arthritis, amyloidosis. Lytic bony destruction or Brodie's abscess in osteomyelitis may also appear as patellar lucencies.

Patellar tumors are uncommon, and the majority are benign [1]. As the patella is considered an epiphyseal equivalent, its most common benign tumors are giant cell tumor (GCT) and chondroblastoma [1,2]. Rarer benign patellar tumors include osteoid osteoma, unicameral bone cyst, aneurysmal bone cyst, and enchondroma [1,2].

Although less common, primary malignant patellar tumors along with patellar metastatic lesions comprise up to one-third of patellar neoplasms, osteosarcoma and chondrosarcoma most frequently encountered [2,3]. Osseous lymphoma, malignant fibrous histiocytoma, and Ewing sarcoma may also occur in the patella [2-6].

Anterior knee pain is the primary clinical symptom of a patellar lesion, with benign etiologies tending towards gradual onset of pain and malignant lesions typically presenting more abruptly [2,7]. Serum inflammatory markers such as erythrocyte sedimentation rate and c-reactive protein may also provide additional information to categorize patellar lesions [8].

Additional information from the clinical history and laboratory values as well as further characterization with cross-sectional imaging are often helpful in narrowing the differential diagnosis. Benign tumors characteristically appear as geographic lesions with a sclerotic rim and sharply defined margins in contrast to malignant tumors with ill-defined borders without a sclerotic rim [2]. In addition, pathologic fractures are more common in malignant patellar tumors [2].

Giant cell tumor

Giant cell tumors are benign osseous tumors that comprise of up to 5% of bony tumors and up to 20% of benign bony tumors [8]. In addition, GCT represent up to 33% of patellar osseous neoplasms [1]. Although classified as benign, GCT may metastasize in up to 9% of cases, with the lungs as the most common site of spread [9].

Patients typically present with knee pain and swelling [2] and are over 20 years old [10].

Radiographs (Figure 1A) demonstrate a radiolucent geographic lesion almost always delineated by a non-sclerotic border [2,10]. GCT on MRI usually demonstrates T1 intermediate signal, T2 hypointensity, and heterogenous enhancement of solid portions [11]. GCT may also contain cystic components and up to 53% of GCT are associated with secondary aneurysmal bone cysts, which contain hemorrhage/fluid components within cystic spaces [12]. Pathologically, osteoclast-like giant cells surrounded by sheets of neoplastic ovoid mononuclear cells are seen [8].

Chondroblastoma

Chondroblastoma is a benign cartilaginous tumor [2,12] with lower prevalence than GCT, as it comprises of less than 1% of bony tumors, less than 3% of benign bony tumors, and approximately 16% of patellar osseous neoplasms [1,13].

Contrary to GCT, chondroblastoma is usually seen in patients younger than the age of 20 [13]. Common presenting clinical symptoms are nonspecific, including pain and joint swelling.

Chondroblastoma on radiograph (Figure 2A) demonstrates a radiolucent geographic lesion outlined most often by a thin sclerotic border [2]. Chondroblastoma on MRI demonstrates a T1 intermediate lobulated lesion with heterogenous enhancement [14]. Similar to GCT, there is an association of chondroblastoma with secondary aneurysmal bone cysts [15]. Pathologically, chondroblasts with chondroid matrix, calcium deposition, and occasional giant cells are appreciated in chondroblastomas.

Osteoid osteoma

Osteoid osteoma is a benign tumor with a central lucent nidus surrounded by sclerosis. The size of an osteoid osteoma is typically less than 1.5 cm, with pathologically similar lesions greater than 2.0 cm classified as osteoblastomas [16]. Osteoid osteomas comprise of up to 5% of patellar osseous tumors [2].

The majority of patients presenting with osteoid osteoma are under the age of 25 [17]. Presenting symptoms are classically described as chronic pain accentuated at nighttime and relieved by non-steroidal analgesics [2].

Osteoid osteoma on radiograph and CT (Figure 3A and C) appears as a well-defined, geographic lesion with a central lucent nidus and surrounding sclerosis [16-19]. Pathologically the central nidus corresponds to osteoblasts and the periphery corresponds to woven bone and peripheral cortical sclerotic reaction [18,19].

Calcium pyrophosphate deposition disease

CPPD, also known as pseudogout, is the deposition of calcium pyrophosphate crystals within fibrocartilage and hyaline cartilage [20]. These crystals subsequently induce inflammatory and degenerative changes within the involved joints [20]. The majority of patients presenting with CPPD are over the age of 65 [21]. Common presenting symptoms include joint pain, swelling, erythema, and decreased range of motion [20,21].

Radiographic findings (Figure 4A) include chondrocalcinosis (the calcification of fibrocartilage and hyaline cartilage), degenerative osteophytosis, joint space narrowing, and subchondral cystic change [20,22]. Prolonged disease may result in osseous erosions [23]. However, the presence of chondrocalcinosis is not specific for CPPD, and may be seen in a variety of diseases, including hyperparathyroidism, degenerative joint disease, gout, and diabetes mellitus [22].

Gout

Gout is the systemic deposition of monosodium urate crystals with associated inflammatory changes around joints and tendons. It is present in up to 4% of the total population [24]. Gout classically presents as sudden monoarthritic pain, most common at the first metatarsophalangeal joint. It has been hypothesized that the predilection for gout at the first metatarsophalangeal joint is due to decreased monosodium urate solubility at the surrounding lower temperature of the foot [25]. Similarly, the superficial location of the patella may also result in a lower temperature that increases the likelihood of gouty tophus formation [25].

Patellar gout has also been associated with history of trauma, bipartite patella, and additional inflammatory disease [25]. Although patellar gout may be seen at both the quadriceps and patellar tendon attachments, the superolateral quadriceps attachment is more common [25].

The erosions of patellar gout on radiograph may mimic a lucent osseous lesion (Figure 5A and 6A), possibly benign and malignant patellar tumors, and other systemic metabolic manifestations, including CPPD and brown tumors from hyperparathyroidism [26]. However MRI will demonstrate characteristic bony erosion with adjacent heterogenous soft tissue extension (Figure 5B-C and 6B-C).

Osteochondral defect

Osteochondral defects represent a localized defect in the articular cartilage and associated subchondral bone [27]. The etiology can be acute secondary to trauma, chronic due to degenerative changes, or postsurgical.

Subchondral cystic changes have been hypothesized to be secondary to the inclusion of synovial fluid into the bony plate via cartilaginous defects of chondrosis [28]. In addition, subchondral marrow edema may also be present secondary to bony microdamage [29]. These cystic changes and marrow edema may simulate lucent areas (Figure 7A) on radiographs [30].

Disseminated Coccidioidomycosis

Coccidioidomycosis is an endemic fungus most prevalent in the Southwestern United States and Central America, as it more effectively survives in regions without significant rainfall or cold temperatures [31]. The spectrum of its disease manifestations ranges from asymptomatic colonization to fulminant disease, partly based on the immune competency of the host [31].

Up to 50% of patients presenting with disseminated disease demonstrate osseous involvement [32]. Although almost any bone in the body may be affected by disseminated coccidioidomycosis, the axial skeleton is more frequently involved [33,34].

Disseminated coccidioidomycosis on radiograph (Figure 8A) typically demonstrates multiple lytic lesions with circumscribed margins [33,34]. In addition, permeative osseous destruction with associated periosteal reaction may also be appreciated [33,34]. The corresponding coccidioidomycosis lesions on CT are usually expansile and hypodense while MRI demonstrates T1 hypointensity, T2 hyperintensity, and contrast enhancement [33].

The differentiation between fungal and bacterial osteomyelitis is often reliant on clinical history due to the relative rarity of fungal osteomyelitis. In general, the imaging appearance of bacterial infection tends to be more aggressive with osteolysis, bony destruction, marrow edema, and periosteal reaction whereas fungal infection demonstrates a more indolent appearance.

Dorsal patellar defect

Dorsal patellar defect is a normal developmental anomaly that at times may be mistaken for pathology. The average age of presentation is 15 years with up to one-third of the cases presenting bilaterally [35]. This lesion is typically seen as an incidental finding, although at times knee pain may be associated. Most dorsal patellar defects resolve spontaneously with gradual sclerotic fill-in [35].

Dorsal patellar defect on radiograph (Figure 9A-B) occurs as a characteristic circumscribed lucency in the superolateral patella with a sclerotic rim [35]. On MRI (Figure 9C-D), there is a corresponding subcortical osseous defect with preserved articular cartilage [35].

Metastatic disease

Metastatic disease to the patella is extremely rare, accounting for less than 0.01% of all osseous tumors [1]. It is even less frequent than primary tumors of the patella [36]. The scarcity of patella metastatic disease may be due in part to its relatively sparse vascular supply [37]. The most common site of primary cancer for patellar metastases is the lung, followed by kidney, colon, and skin [36]. Squamous cell carcinoma and adenocarcinoma are the most common subtypes for primary lung cancer with metastases to the patella [36].

Radiographic features of patellar metastases depend on the primary cancer. Common findings include lytic lesions (Figure 10) with possible superimposed pathologic fracture and periosteal reaction [36]. However, imaging may be insufficient to differentiate between primary patella tumor and metastatic disease, and biopsy may be required.

Postoperative change

Sutures through trans-osseous patellar bone tunnels is one of the main techniques for the current repair of acute quadriceps tendon rupture [38]. Figure 12 illustrates a schematic for the trans-osseous tunnels traversing the patella in a longitudinal direction. Quadriceps tendon rupture usually occurs in patients over the age of 40 and in patients with predisposing factors including chronic steroid therapy, diabetes mellitus, and systemic lupus erythematosus [39]. Complications after trans-osseous suture repair include re-injury of the quadriceps tendon, postoperative patellar stress fractures, and additional general postoperative complications such as infection and deep venous thrombosis [40].

An anterior exit direction of trans-osseous patellar drill holes has been hypothesized to increase the risk of postoperative patellar fracture, although studies to evaluate this have been limited [40]. In addition, longitudinal patellar drill holes may have increased stress due to their increased length [40].

Postoperative cystic expansion adjacent to the trans-osseous tunnels (Figure 11) or the tunnels themselves may simulate a lucent patellar lesion on radiographs. Surgical history or further investigation on cross-sectional imaging may assist in making the diagnosis.

TEACHING POINT

A radiographically lucent patellar lesion may represent a variety of etiologies, ranging from more commonly seen degenerative, metabolic, infectious, developmental, posttraumatic, postoperative causes to rarer benign and malignant neoplasms. Radiographic features such as circumscribed borders and sharply delineated margins favor benign lesions while ill-defined margins suggest malignant etiologies.

REFERENCES

1. Mercuri M, Casadei R. Patellar tumors. Clin Orthop Relat Res. 2001 Aug;(389):35-46. PMID 11501820

2. Song M, Zhang Z, Wu Y, Ma K, Lu M. Primary tumors of the patella. World J Surg Oncol. 2015;13:163. PMID 25906772

3. Ehara, S., Khurana, J. S., Kattapuram, S. V., Rosenberg, A. E., El-Khoury, G. Y., & Rosenthal, D. I. (1989). Osteolytic lesions of the patella. American Journal of Roentgenology, 153(1), 103-106. PMID 2735276

4. Chandra A, Eilender D. Uncommon sites of presentation of hematologic malignancies. Case 1: localized primary non-

Hodgkin's lymphoma of the patella. J Clin Oncol. 1999;17:1640-2. PMID 10334554

5. López-Barea F, Rodríguez-Peralto JL, Burgos-Lizalde E, González-López J, Sánchez-Herrera S. Case report 639: malignant fibrous histiocytoma (MFH) of the patella. Skeletal Radiol. 1991;20:125-8. PMID 1850554

6. Gorelik N, Dickson BC, Wunder JS, Bleakney R. Ewing's sarcoma of the patella. Skeletal Radiol. 2013;42:729-33. doi: 10.1007/s00256-013-1580-0. PMID 23381466

7. Ferguson PC, Griffin AM, Bell RS. Primary patellar tumors. Clin Orthop Relat Res. 1997;336:199-204. PMID 9060506

8. Achmad Kamal F, Errol U. Hutagalung, Saukani Gumay, Yogi Prabowo, Yanuarso Yanuarso. Primary malignant giant cell tumor of the patella: report of a rare case. Med J Indonesia. 2013;22:238-42.

9. Qureshi SS, Puri A, Agarwal M, Desai S, Jambhekar N. Recurrent giant cell tumor of bone with simultaneous regional lymph node and pulmonary metastases. Skeletal Radiol. 2005 Apr;34(4):225-8. PMID 15365782

10. Stacy G, Peabody T, Dixon L. Mimics on Radiography of Giant Cell Tumor of Bone. AJR Am J Roentgenol. 2003;181(6):1583-9. PMID 14627578

11. Pereira H, Marchiori E, Severo A. Magnetic Resonance Imaging Aspects of Giant-Cell Tumours of Bone. J Med Imaging Radiat Oncol. 2014;58(6):674-8. PMID 25256094

12. Tan H, Yan M, Yue B, Zeng Y, Wang Y. Chondroblastoma of the patella with aneurysmal bone cyst. Orthopedics. 2014;37:e87-91. PMID 24683664

13. Erickson JK, Rosenthal DI, Zaleske DJ et-al. Primary treatment of chondroblastoma with percutaneous radio-frequency heat ablation: report of three cases. Radiology. 2001;221 (2): 463-8. PMID 11687691

14. Kaim AH, Hügli R, Bonél HM, Jundt G. Chondroblastoma and clear cell chondrosarcoma: radiological and MRI characteristics with histopathological correlation. Skeletal radiology. 2002. 31 (2): 88-95. PMID 11828329

15. Mankin HJ, Hornicek FJ, Ortiz-cruz E et-al. Aneurysmal bone cyst: a review of 150 patients. J. Clin. Oncol. 2005;23 (27): 6756-62. PMID 16170183

16. Eisenberg RL. Bubbly lesions of bone. AJR Am J Roentgenol. 2009;193 (2): W79-94. PMID 19620421

17. Dookie AL, Joseph RM. Osteoid Osteoma. [Updated 2021 Aug 25]. In: StatPearls [Internet]. Treasure Island (FL): StatPearls Publishing; 2021 Jan-. PMID 30725964

18. Ma K, Zhao HT, Niu XH, Zhang Q. Osteoid osteoma of the patella: report of two cases. Chin Med J (Engl). 2011 Dec;124(23):4096-8. PMID 22340349

19. Carneiro BC, Da Cruz IAN, Ormond Filho AG, et al. Osteoid osteoma: the great mimicker. Insights Imaging. 2021;12(1):32. Published 2021 Mar 8. PMID 33683492

20. Iqbal SM, Qadir S, Aslam HM, Qadir MA. Updated Treatment for Calcium Pyrophosphate Deposition Disease: An Insight. Cureus. 2019;11(1):e3840. PMID 30891381

21. Zamora EA, Naik R. Calcium Pyrophosphate Deposition Disease. [Updated 2021 Jul 20]. In: StatPearls [Internet]. Treasure Island (FL): StatPearls Publishing; 2022 Jan-. Available from: https://www.ncbi.nlm.nih.gov/books/NBK540151/

22. McQueen FM, Doyle A, Dalbeth N. Imaging in the crystal arthropathies. Rheumatic diseases clinics of North America. 2014;40(2):231-49. PMID 24703345

23. Mank VMF, Goldstein E, Babb S, Meghpara S, Breighner C, Roberts J. 20 Years of Radiographic Imaging: Crystalline Deposits Causing Severe Arthropathy and Erosions. Mil Med. 2021 Apr 7:usab129. PMID 33826727

24. Ragab G, Elshahaly M, Bardin T. Gout: An old disease in new perspective - A review. J Adv Res. 2017;8(5):495-511. 2017.04.008. PMID 28748116

25. Chiu MK, Lewis NA. Intraosseous gout mimicking giant cell tumor of the patella. Skeletal Radiol. 2020 Aug;49(8):1325-1328. PMID 32236660

26. Hopper G, Gupta S, Bethapudi S, Ritchie D, Macduff E, Mahendra A. Tophaceous gout of the patella: a report of two cases. Case Rep Rheumatol. 2012;2012:253693. PMID 23198243

27. Gorbachova T, Melenevsky Y, Cohen M, Cerniglia BW. Osteochondral Lesions of the Knee: Differentiating the Most Common Entities at MRI. Radiographics. 2018 Sep-Oct;38(5):1478-1495. PMID 30118392

28. Han SH, Lee JW, Lee DY, Kang ES. Radiographic changes and clinical results of osteochondral defects of the talus with and without subchondral cysts. Foot Ankle Int. 2006 Dec;27(12):1109-14. PMID 17207440

29. Li G, Yin J, Gao J, et al. Subchondral bone in osteoarthritis: insight into risk factors and microstructural changes. Arthritis Res Ther. 2013;15(6):223. PMID 24321104

30. Sanders RK, Crim JR. Osteochondral injuries. Semin Ultrasound CT MR. 2001 Aug;22(4):352-70. PMID 11513159

31. Stockamp NW, Thompson GR 3rd. Coccidioidomycosis. Infect Dis Clin North Am. 2016 Mar;30(1):229-46. PMID 26739609

32. McGahan JP, Graves DS, Palmer PE, et al. Classic and contemporary imaging of coccidioidomycosis. AJR Am J Roentgenol. 1981;136: 393-404. PMID 6781265

33. Zeppa MA, Laorr A, Greenspan A, et al. Skeletal coccidioidomycosis: imaging findings in 19 patients. Skeletal Radiol. 1996;25:337-343. PMID 8737998

34. Gupta NA, Iv M, Pandit RP, Patel MR. Imaging manifestations of primary and disseminated coccidioidomycosis. Applied Radiology. The Journal of Practical Medical Imaging Management. 2015.

35. Safran MR, McDonough P, Seeger L, Gold R, Oppenheim WL. Dorsal defect of the patella. J Pediatr Orthop. 1994 Sep-Oct;14(5):603-7. PMID 7962501

36. Li G, Shan C, Sun R, et al. Patellar metastasis from primary tumor. Oncol Lett. 2018;15(2):1389-1396. PMID 29434829

37. Scapinelli R. Blood supply of the human patella. Its relation to ischaemic necrosis after fracture. J Bone Joint Surg Br. 1967 Aug;49(3):563-70. PMID 6037574

38. Sherman, S. L., Copeland, M. E., Milles, J. L., Flood, D. A., & Pfeiffer, F. M. (2016). Biomechanical Evaluation of Suture Anchor Versus Transosseous Tunnel Quadriceps Tendon Repair Techniques. Arthroscopy: The Journal of Arthroscopic & Related Surgery, 32(6), 1117-1124. PMID 26895785

39. Calvo E, Ferrer A, Robledo AG, Alvarez L, Castillo F, Vallejo C. Bilateral simultaneous spontaneous quadriceps tendons rupture. A case report studied by magnetic resonance imaging. Clin Imaging. 1997 Jan-Feb;21(1):73-6. PMID 9117937

40. Gregory JM, Sherman SL, Mather R, Bach BR Jr. Patellar stress fracture after transosseous extensor mechanism repair: report of 3 cases. Am J Sports Med. 2012 Jul;40(7):1668-72. PMID 22508427

FIGURES

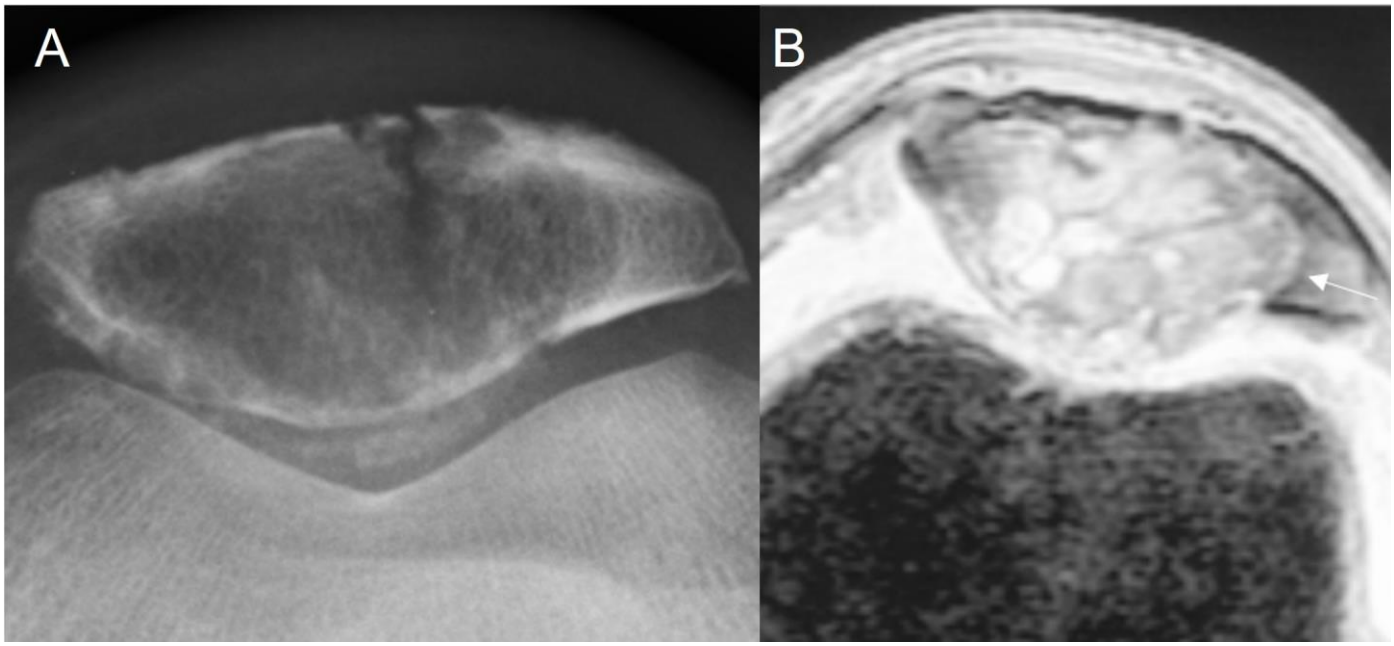

Figure 1: *Giant Cell Tumor*
85-year-old male with history of prostate cancer and gout with patellar giant cell tumor demonstrated on biopsy. He presented with 4 weeks of left knee pain without history of trauma.

Findings:
Expansile lucent patellar lesion with narrow zone of transition (arrow) and a minimally displaced pathologic fracture through the lesion.

Technique:
A) Sunrise view left knee radiograph and B) Left knee axial T1 MRI (GE Signa 1.5T; TR 3500; TE 17; slice thickness 4 mm; without contrast).

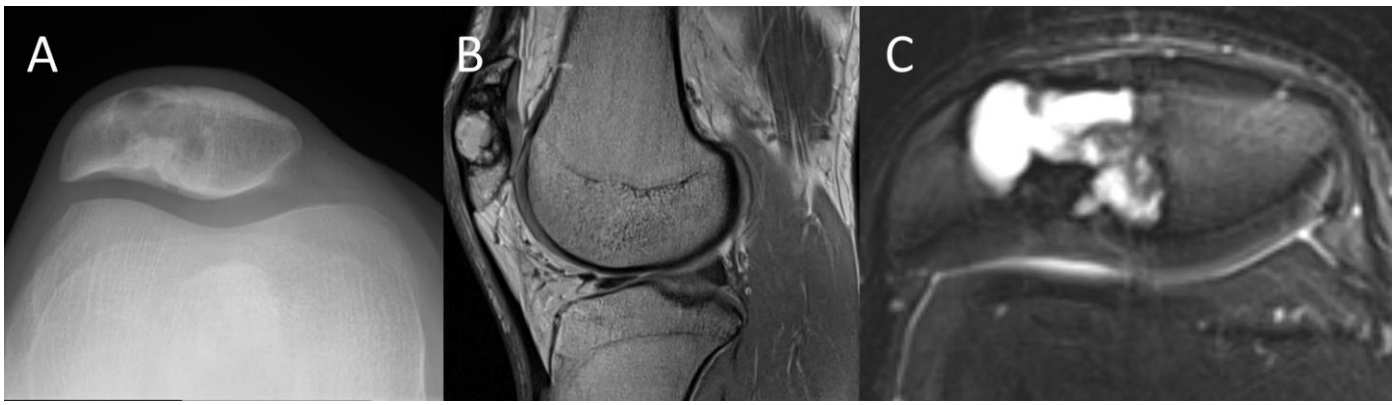

Figure 2: *Chondroblastoma*
26-year-old male with gradual onset right knee pain with patellar chondroblastoma shown on biopsy.

Findings: Patellar geographic multilobulated lytic lesion with narrow zone of transition and sclerotic border. There is endosteal scalloping along the anterior cortex of the patella.

Technique: A) Right knee sunrise radiograph. B and C) Right knee proton-density sagittal and T2 axial fat-suppressed MRI (Siemens Skyra 3T; sagittal proton-density - TR 2240; TE 12; slice thickness 3 mm; and axial T2 - TR 4890; TE 73; slice thickness 3 mm; without contrast).

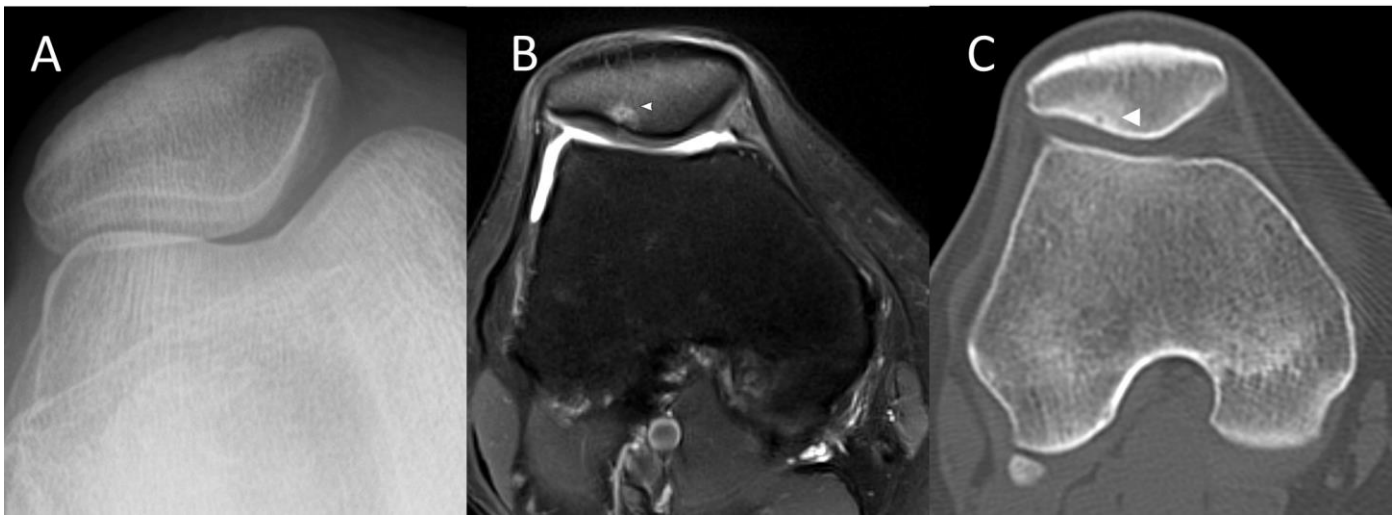

Figure 3: *Osteoid Osteoma*
33-year-old female with right knee pain for a few months and imaging findings consistent with osteoid osteoma.

Findings: Subtle subchondral sclerosis along the lateral patellar facet on radiograph that corresponds to a focal subchondral area of edema on MRI and demonstrated a punctate lucency within subchondral bony sclerosis on CT consistent with an osteoid osteoma.

Technique: A) Right knee sunrise radiograph. B) Axial T2 fat-suppressed MR of the right knee (Siemens Skyra 3T; TR 3700; TE 53; slice thickness 3 mm; without contrast). C) Axial CT of the right knee (Siemens Sensation; kVp 120; mA 406; slice thickness 3 mm; without contrast).

Figure 4: *Metabolic disease - Calcium Pyrophosphate Deposition Disease*
69-year-old female with 2-week history of lateral knee pain without trauma and imaging findings consistent with calcium pyrophosphate deposition disease.

Findings: Chondrocalcinosis with lucent irregularity along the lateral patella (arrow) that corresponds to focal erosion on MRI. Findings are consistent with calcium pyrophosphate deposition disease.

Technique: A) Left knee sunrise radiograph. B) Left knee axial T2 fat-suppressed MRI (GE Signa Architect 3T; TR 5555; TE 122; slice thickness 4 mm; without contrast).

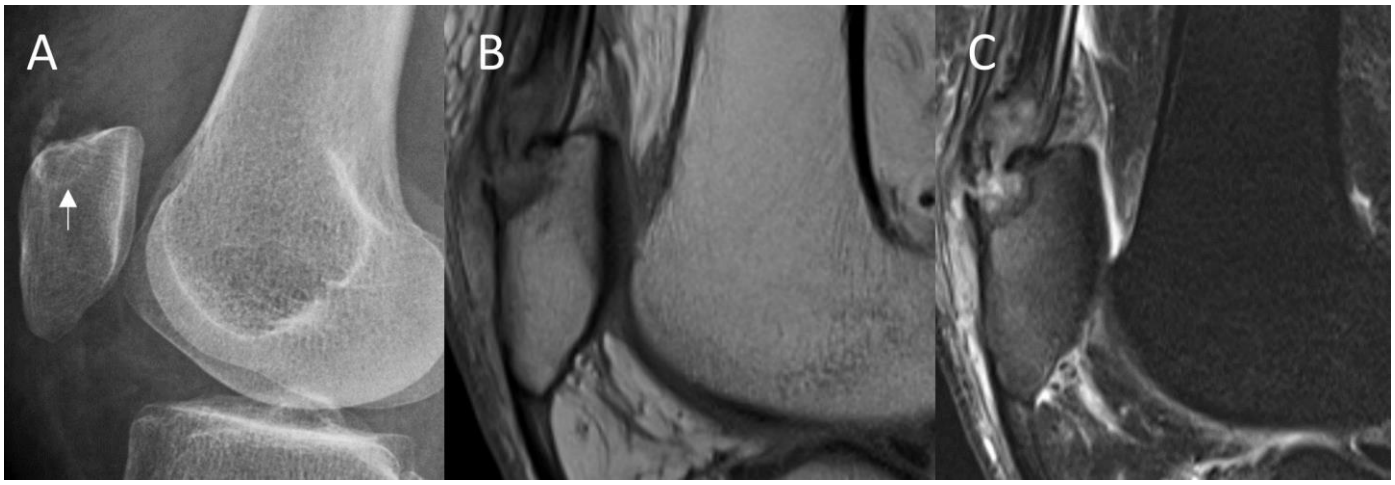

Figure 5: Gout
78-year-old female with history of gout presenting with left knee pain and imaging findings consistent with gout.

Findings: Subtle lucency along the superior patella (arrow) with adjacent mineralization. Corresponding erosion seen on MRI with heterogenous material extending from the area of erosion into the distal quadriceps tendon and prepatellar bursa compatible with tophaceous gout.

Technique: A) Lateral left knee radiograph. B and C) Sagittal proton-density and sagittal T2 fat-suppressed left knee MRI (Siemens Skyra 3T; sagittal proton-density - TR 2000; TE 10; slice thickness 4 mm; and sagittal T2- TR 3700; TE 57; slice thickness 4 mm; without contrast).

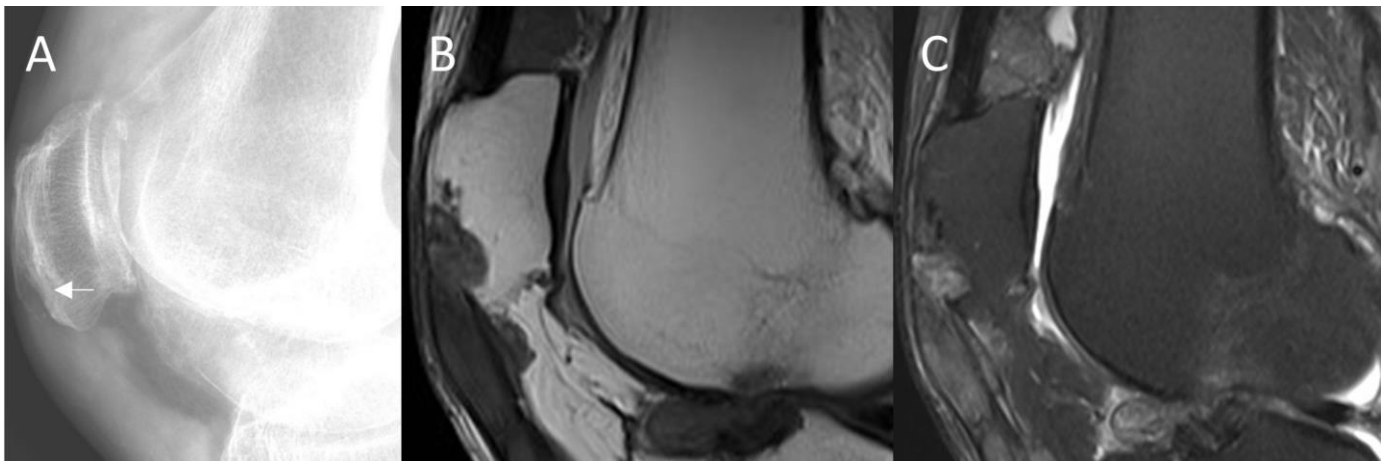

Figure 6: Gout
71-year-old male with right knee pain and imaging findings consistent with gout.

Findings: Subtle lucent area about the anteroinferior patella (arrow) that corresponds to erosive changes at the attachment of the patellar tendon and heterogenous material extending from the area of bony erosion into the proximal patellar tendon compatible with tophaceous gout.

Technique: A) Lateral right knee radiograph. B and C) Sagittal proton-density and T2 MRI of the right knee (Siemens Skyra 3T; sagittal proton density - TR 3000; TE 34; slice thickness 3 mm; and sagittal T2 - TR 3600; TE 94; slice thickness 3 mm; without contrast).

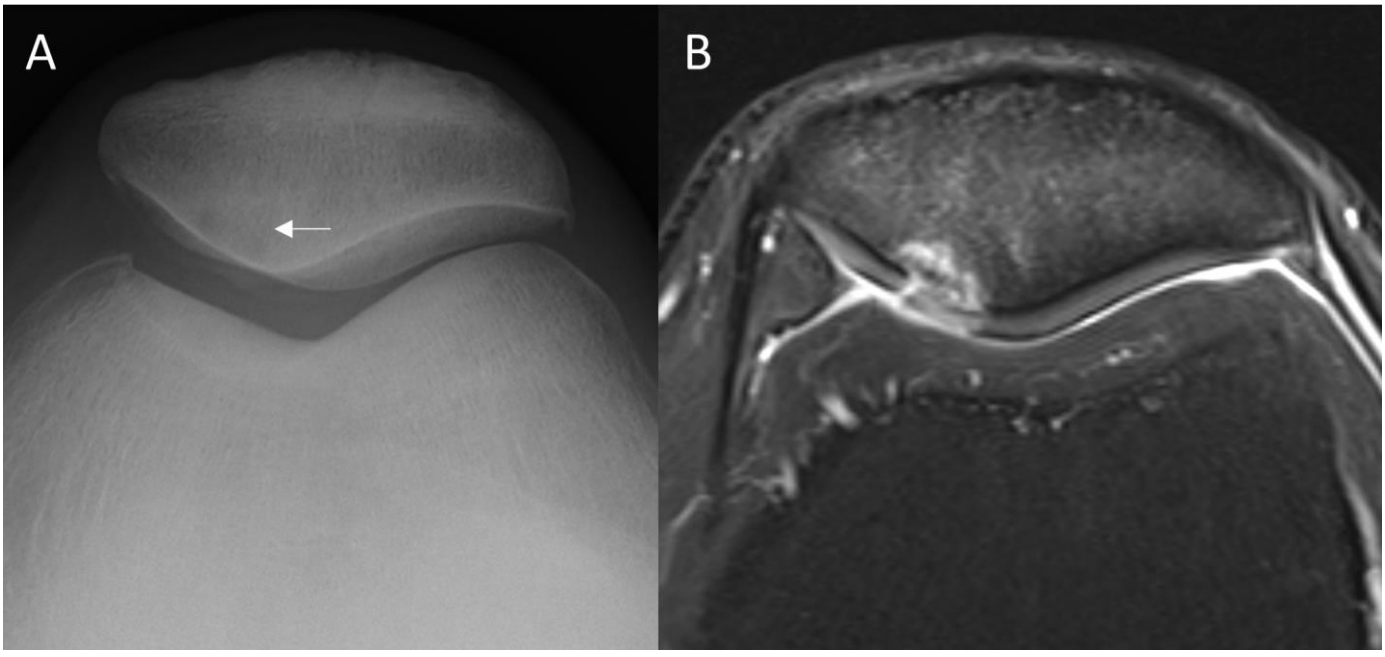

Figure 7: *Degenerative change - Osteochondral defect*
55-year-old male presenting with gradual onset left knee pain and imaging findings consistent with an osteochondral defect.

Findings: Subchondral lucency within the medial patellar facet, without significant joint space narrowing. Corresponding full-thickness osteochondral defect within the medial patellar facet with surrounding reactive edema.

Technique: A) Left knee sunrise radiograph. B) Axial T2 fat-suppressed MRI of the left knee (Siemens Skyra 3T; TR 4780; TE 71; slice thickness 4 mm; without contrast).

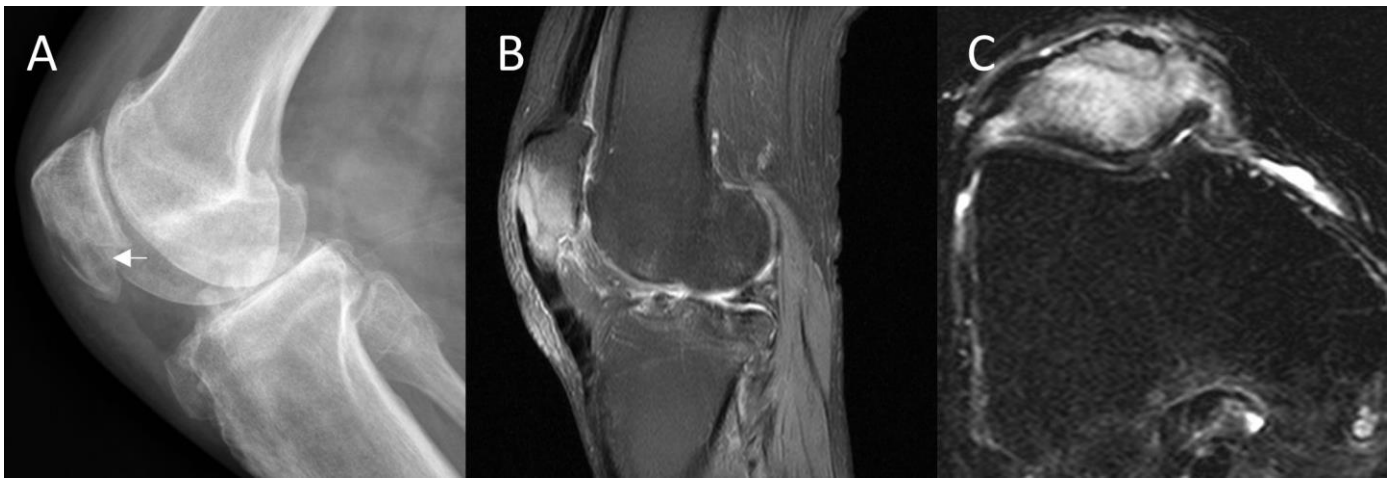

Figure 8: *Infectious disease - Disseminated Coccidioidomycosis*
60-year-old male with history of coccidioidomycosis fungemia presenting with right knee pain and imaging findings consistent with osseous coccidioidomycosis.

Findings: Lucent area about the anteroinferior patella (arrow) that corresponds to a T2 hyperintense lesion with exuberant surrounding marrow edema compatible with disseminated fungal infection.

Technique: A) Lateral right knee radiograph. B and C) Sagittal and axial T2 fat-suppressed MRI of the right knee (Siemens Sonata 1.5T; sagittal T2 - TR 3230; TE 85; slice thickness 4 mm; and axial T2 - TR 5720; TE 91; slice thickness 4 mm; without contrast).

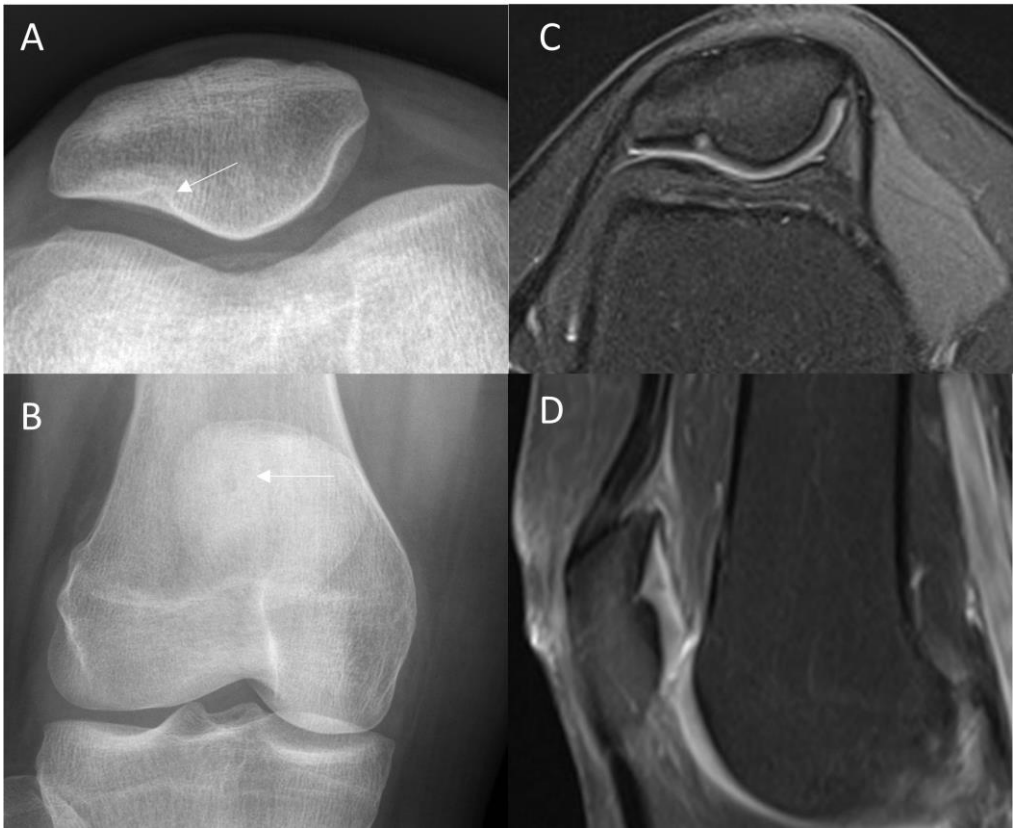

Figure 9: *Developmental variant - Dorsal patellar defect*
31-year-old female with history of right knee pain with imaging findings consistent with dorsal patellar defect.

Findings: Lucent area with a sclerotic rim within the subcortical lateral patella facet (arrow) that corresponds to a subcortical bone plate irregularity with preserved overlying cartilage consistent with dorsal patellar defect.

Technique: A and B) Sunrise and AP right knee radiographs. C and D) Axial T2 and sagittal proton density fat-suppressed MRI of the right knee (Siemens Skyra 3T; axial T2 - TR 4660; TE 63; slice thickness 4 mm; and sagittal proton density - TR 3500; TE 10; slice thickness 3 mm; without contrast).

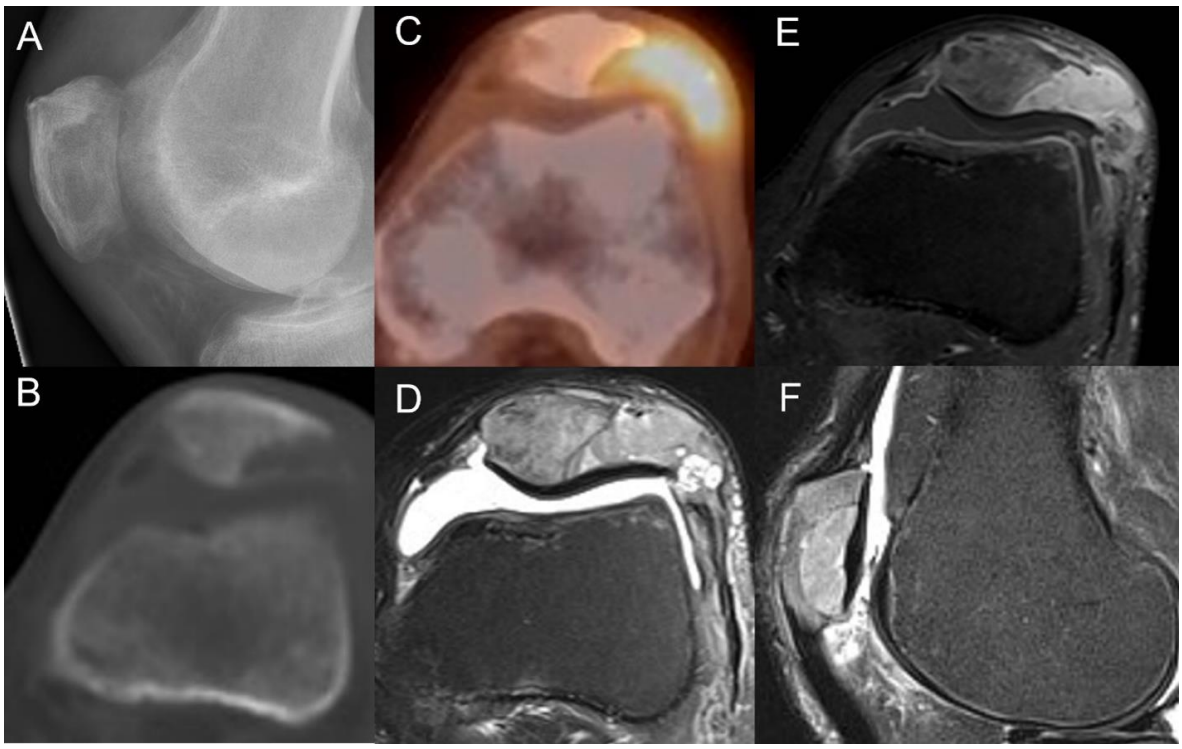

Figure 10: *Metastatic disease*
60-year-old male with history of metastatic lung adenocarcinoma with right knee pain and metastatic lung adenocarcinoma of the patella shown on biopsy.

Findings: Ill-defined lucent area within the lateral patella that corresponds to a lytic lesion with wide zone of transition and increased F18-FDG uptake (SUV max 6.7) on PET/CT. MRI demonstrates an expansile, enhancing mass with associated cortical loss and extraosseous soft tissue extension.

Technique: A) Lateral right knee radiograph. B and C) Axial PET/CT (Siemens Biograph; 8.5 mCi F18-FDG; 45 minutes injection time; kVp 120; mA 201; slice thickness 3 mm; without contrast). D and E) Axial T2 fat-suppressed and contrast enhanced T1 fat-suppressed MRI of the right knee (Siemens Aera 1.5T; axial T2 - TR 5580; TE 84; slice thickness 3 mm; and contrast enhanced T1 - TR 600; TE 18; slice thickness 3 mm; 7.5 mL Gadobutrol). F) Sagittal T2 fat-suppressed MRI of the right knee (Siemens Aera 1.5T; TR 4330; TE 84; slice thickness 3 mm; 7.5 mL Gadobutrol).

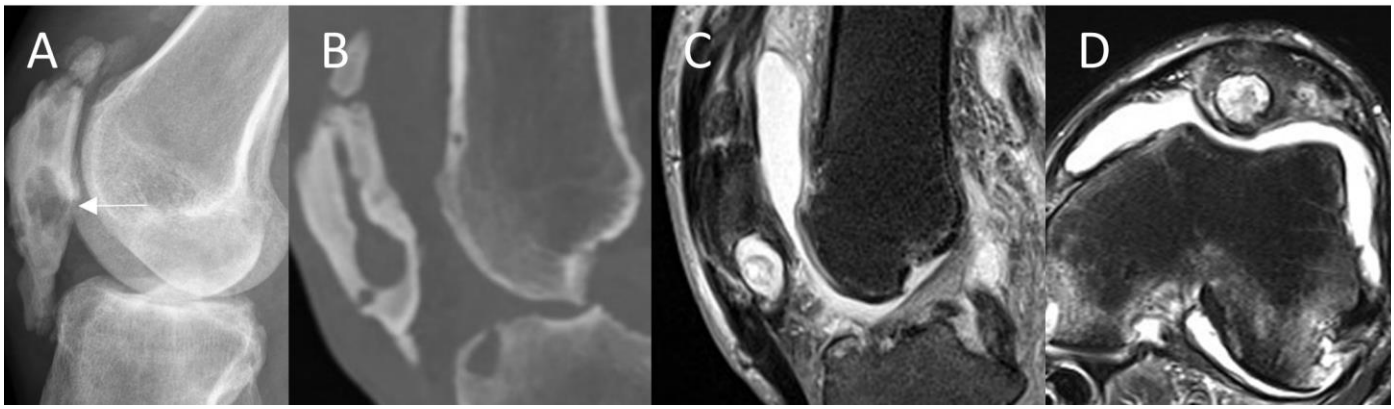

Figure 11: *Postoperative change - Status post quadriceps tendon repair with trans-osseous patellar bone tunnels sutures*
59-year-old male with history of right quadriceps tendon repair approximately twenty years prior presenting with knee pain with imaging findings consistent with postoperative changes.

Findings: Lucent area within the posteroinferior patella (arrow) that corresponds to intraosseous cystic changes around the repair sutures seen on both CT and MRI.

Technique: A) Lateral right knee radiograph. B) Sagittal CT of the right knee (Siemens SOMATOM Force; kVp 120; mA 66; slice thickness 1 mm; 100 mL Iodixanol). C and D) Sagittal T2 and Axial T2 fat-suppressed MRI of the right knee (Siemens Aera 1.5T; sagittal T2 - TR 4330; TE 90; slice thickness 3 mm; and axial T2 - TR 5580; TE 84; slice thickness 4 mm; without contrast).

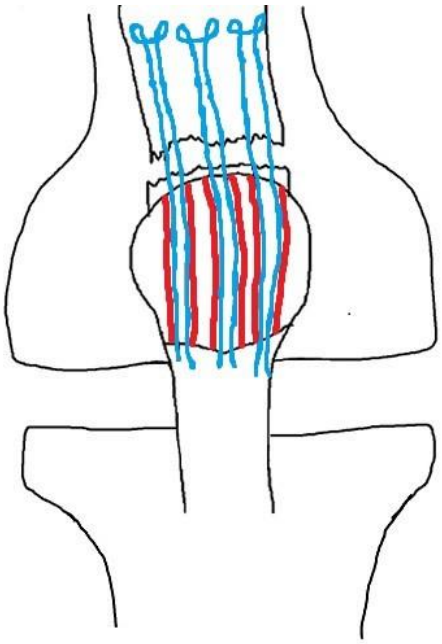

Figure 12 (left): Illustration for trans-osseous tunnels (red) and sutures (blue) in the setting of quadriceps tendon repair.

Diagnosis	Clinical presentation	Radiograph findings	CT findings	MRI findings
Giant cell tumor	Knee pain and swelling. Typically over the age of 20.	Lucent geographic lesion with non-sclerotic border.	Lucent geographic lesion with non-sclerotic border.	T1 intermediate. T2 hypointense. Heterogenous enhancement of solid portions.
Chondroblastoma	Knee pain and swelling. Typically under the age of 20.	Lucent geographic lesion with thin sclerotic border.	Lucent geographic lesion with thin sclerotic border.	T1 intermediate. T2 variable. Heterogenous enhancement.
Osteoid Osteoma	Chronic knee pain accentuated at nighttime and relieved by non-steroidal analgesics. Typically under the age of 25.	Well-defined, geographic lesion with a central lucent nidus and surrounding sclerosis.	Well-defined, geographic lesion with a central lucent nidus and surrounding sclerosis.	Nonspecific.
CPPD	Knee pain and swelling. Typically over the age of 65.	Chondrocalcinosis, degenerative osteophytosis, joint space narrowing, and subchondral cystic change.	Chondrocalcinosis, focal erosion, degenerative osteophytosis, joint space narrowing, and subchondral cystic change.	Focal erosion.
Gout	Acute monoarthritic pain.	Focal lucent area and chondrocalcinosis.	Focal erosion and chondrocalcinosis.	Focal erosion.
Osteochondral Defect	Can be degenerative or secondary to trauma.	Focal lucent area with possible subchondral sclerosis.	Focal lucent area with possible subchondral sclerosis.	Focal lucent area with possible subchondral edema.
Disseminated infection	Coccidioidomycosis more frequently involves the axial skeleton.	Multiple lucent lesions with circumscribed margins.	Expansile and hypodense lesions.	T1 hypointense. T2 hyperintense. Variable enhancement. Marked surrounding edema.
Dorsal patellar defect	Possible knee pain Average age of presentation of 15. One-third of cases are bilateral.	Characteristic circumscribed lucency in the superolateral patella with a sclerotic rim.	Characteristic circumscribed lucency in the superolateral patella with a sclerotic rim.	Subcortical osseous defect with preserved articular cartilage.
Metastatic disease	Extremely rare. Most common primaries include lung, renal, colon, and melanoma.	Lytic/sclerotic lesion depending on primary malignancy with possible pathologic fracture and periosteal reaction.	Lytic/sclerotic lesion depending on primary malignancy with possible pathologic fracture and periosteal reaction.	Variable depending on primary malignancy.
Intraosseous tendon repair with cystic postoperative change	History of surgery. Quadriceps tendon rupture usually occur in patients over the age of 40.	May mimic lucent lesion on radiograph.	Postoperative changes.	Postoperative changes.

Table 1: Summary table of lucent patellar lesions.

ABBREVIATIONS

CPPD = Calcium pyrophosphate deposition disease
CT = Computed tomography
GCT = Giant cell tumor
MRI = Magnetic resonance imaging

KEYWORDS

Patella; MRI; CT; giant cell tumor; chondroblastoma; osteoid osteoma; gout; osteochondral defect; disseminated coccidioidomycosis; metastases; dorsal patellar defect